

1 **Scaling diagnostics in times of COVID-19: Rapid prototyping of 3D-**
2 **printed water circulators for Loop-mediated Isothermal Amplification**
3 **(LAMP) and detection of SARS-CoV-2 virus**

4
5 Everardo González-González^{1,2}, Itzel Montserrat Lara-Mayorga^{1,3}, Andrés García-Rubio^{1,3},
6 Carlos Ezio Garciaméndez-Mijares^{1,3}, Gilberto Emilio-Guerra-Alvarez^{1,3}, Germán García-
7 Martínez^{1,3}, Juan Aguayo^{1,3}, Yu Shrike Zhang⁴, Sergio Omar Martínez-Chapa^{3,*}, Grissel
8 Trujillo-de Santiago^{1,3,*}, Mario Moisés Alvarez^{1,2*}

9
10 ¹ Centro de Biotecnología-FEMSA, Tecnológico de Monterrey, CP 64849, Monterrey,
11 Nuevo León, México

12 ² Departamento de Bioingeniería, Tecnológico de Monterrey, CP 64849, Monterrey, Nuevo
13 León, México

14 ³ Departamento de Ingeniería Mecatrónica y Eléctrica, Tecnológico de Monterrey, CP
15 64849, Monterrey, Nuevo León, México

16 ⁴ Division of Engineering in Medicine, Department of Medicine, Brigham and Women's
17 Hospital, Harvard Medical School, Cambridge 02139, MA, USA

18 *Corresponding authors. E-mails: mario.alvarez@tec.mx; grissel@tec.mx

19

20

21

22

23 **Abstract**

24 By the first week of April 2020, more than 1,500,000 positive cases of COVID-19 and
25 more than 50,000 deaths had been officially reported worldwide. While developed
26 countries such as the USA, Italy, England, France, Spain, and Germany struggle to mitigate
27 the propagation of SARS-CoV-2, the COVID-19 pandemic arrived in Latin America, India,
28 and Africa—territories in which the mounted infrastructure for diagnosis is greatly
29 underdeveloped. An actual epidemic emergency does not provide the required timeframe
30 for testing new diagnostic strategies; therefore, the first line of response must be based on
31 commercially and readily available resources. Here, we demonstrate the combined use of a
32 three-dimensional (3D)-printed incubation chamber for commercial Eppendorf PCR tubes,
33 and a colorimetric embodiment of a loop-mediated isothermal amplification (LAMP)
34 reaction scheme for the detection of SARS-CoV-2 nucleic acids. We used this strategy to
35 detect and amplify SARS-CoV-2 DNA sequences using a set of in-house designed
36 initiators that target regions encoding the N protein. We were able to detect and amplify
37 SARS-CoV-2 nucleic acids in the range of ~625 to 2×10^5 DNA copies by this
38 straightforward method. The accuracy and simplicity of this diagnostics strategy may
39 provide a cost-efficient and reliable alternative for use during the COVID-19 pandemics,
40 particularly in underdeveloped regions where the availability of RT-qPCR instruments may
41 be limited. Moreover, the portability, ease of use, and reproducibility of this strategy make
42 it a reliable alternative for deployment of point-of-care SARS-CoV-2 detection efforts
43 during the pandemics.

44

45 **Key words:** LAMP, point-of-care, SARS-CoV-2, COVID-19, diagnostic, portable,
46 isothermal nucleic acid amplification

47

48 **Introduction**

49 By the end of the first week of April 2020, more than one and a half million positive cases
50 of COVID-19 were officially reported across the globe[1]. Even developed countries, such

51 as the USA, England, France, and Germany, are struggling to mitigate the propagation of
52 SARS-CoV-2 by implementing social distancing and widespread testing. Less developed
53 regions, such as Latin America, India, and Africa, are now experiencing the arrival of
54 COVID-19, but these—territories are woefully lacking in the finances or the mounted
55 infrastructure for diagnosis of this pandemic infection. Rapid and massive testing of
56 thousands of possibly infected subjects has been an important component of the strategy of
57 the countries that are effectively mitigating the spreading of COVID-19 among their
58 populations (i.e., China[2], South Korea [3], and Singapore [4]). By comparison,
59 developing countries with high demographic densities, such as México [5], India [6], or
60 Brazil [7], may not be able to implement a sufficient number of centralized laboratories for
61 rapid large-scale testing for COVID-19.

62 Many methodologies have been proposed recently to deliver cost-effective diagnosis (i.e.,
63 those based on immunoassays [8–11] or specific gene hybridization assisted by CRISPR-
64 Cas systems [12–14]). While immunoassays are an accurate and efficacious tool for
65 assessing the extent of the infection for epidemiological studies [15], their usefulness is
66 limited to the identification of infected subjects during early phases of infection [11,16], a
67 critical period for infectiveness. For instance, experimental evidence collected from a small
68 number of COVID-19 patients (9 subjects) showed that 100% of them produced specific
69 immunoglobulins G (IgGs) for SARS-CoV-2 within two weeks of infection, but only 50%
70 of them did during the first week post infection [17].

71 Nucleic acid amplification continues to be the gold standard for the detection of viral
72 diseases in the early stages [18–22], and very small viral loads present in symptomatic or

73 asymptomatic patients can be reliably detected using amplification based technics, such as
74 PCR[23–25], RPA[26], and LAMP[27–29].

75 During the last two pandemic events with influenza A/H1N1/2009 and COVID-19, the
76 Centers for Disease Control (CDC) and the World Health Organization (WHO)
77 recommended real-time quantitative PCR (RT-qPCR) methods as the gold standard for
78 official detection of positive cases[16,30]. However, the reliance on RT-qPCR often leads
79 to dependence on centralized laboratory facilities for testing [16,30–33]. To resolve this
80 drawback, isothermal amplification reaction schemes (i.e., loop-mediated isothermal
81 amplification (LAMP) and recombinase polymerase amplification (RPA)) have been
82 proposed as alternatives to PCR-based methods and devices for point-of-care settings
83 [32,34,35]. The urgency of using reliable molecular-based POC methods for massive
84 diagnostic during epidemiological emergencies has become even more evident during the
85 current COVID-19 pandemics [30,36,37].

86 In these times of COVID-19 [38], scientists and philanthropists around the globe have
87 worked expeditiously on the development of rapid and portable diagnostics for SARS-
88 CoV-2. Several reports have demonstrated the use of colorimetric LAMP-based methods
89 for diagnosis of pandemic COVID-19 [39–44]. Some of these reports (currently available
90 as preprints) use phenol red, a well-known pH indicator, to assist in the visual
91 discrimination between positive and negative samples [39,40].

92 In this study, we demonstrate the use of a simple embodiment of a colorimetric Loop-
93 mediated Isothermal amplification (LAMP) protocol for the detection and amplification of
94 synthetic samples of SARS-CoV-2, the causal viral agent of COVID-D. In this LAMP-
95 based strategy, also assisted by the use of phenol red, sample incubation is greatly

96 facilitated by the use of a three-dimensional (3D)-printed incubator connected to a
97 conventional water circulator, while discrimination between positive and negative samples
98 is achieved by visual inspection. We quantitatively analyze differences in color between
99 positive and negative samples using color decomposition and analysis in the color CIELab
100 space[45]. Moreover, we compare the sensibility of this LAMP colorimetric method versus
101 PCR protocols. This simple strategy is potentially adequate for the fast deployment of
102 diagnostic efforts in the context of COVID-19 pandemics.

103

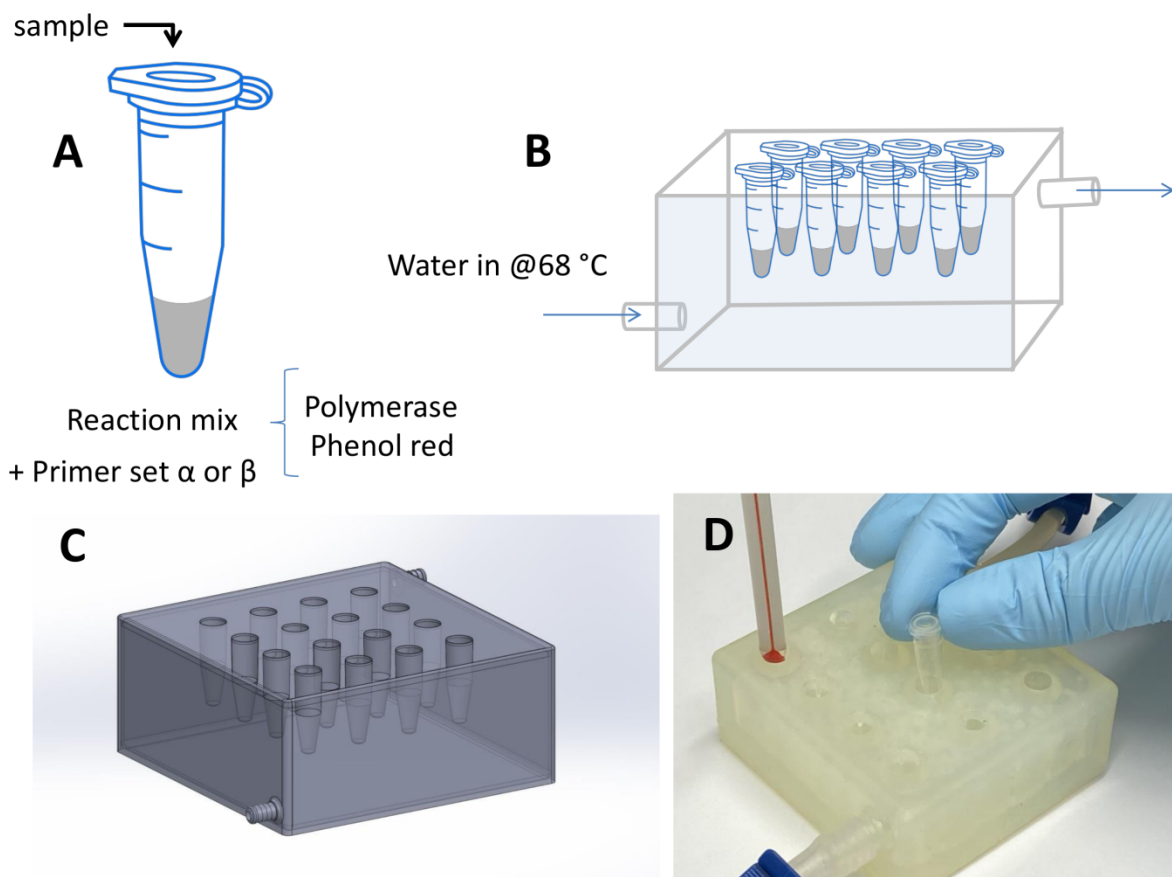
104 **Materials and Methods**

105 *Equipment specifications:* We ran several hundred amplification experiments using a
106 colorimetric LAMP method in a 3D-printed incubation chamber designed in house and
107 connected to a conventional water circulator (Figure 1). The design and all dimensional
108 specifications of this chamber have been made available in Supplementary Information
109 (Figure S1,S2; Supplementary File S1). In the experiments reported here, we used a
110 chamber with dimensions of $20 \times 5 \times 15 \text{ cm}^3$ and a weight of 0.4 kg (without water). A
111 conventional water circulator (WVR, PA, USA), was used to circulate hot water (set point
112 value at 76 °C) through the 3D-printed chamber for incubation of the Eppendorf PCR tubes
113 (0.2 mL). In this first chamber prototype, twelve amplification reactions can be run in
114 parallel. This concept design is amenable for fabrication in any STL-3D printing platform
115 and may be scaled up to accommodate a larger number of tubes.

116 We used a blueGel electrophoresis unit, powered by 120 AC volts, to validate the LAMP
117 amplification using gel electrophoresis. Photo-documentation was done using a
118 smartphone camera. We also used a Synergy HT microplate reader (BioTek Instruments,

119 VT, USA) to detect the fluorescence induced by an intercalating reagent in positive
120 samples from the PCR reactions.

121 *Validation DNA templates:* We used plasmids containing the complete N gene from 2019-
122 nCoV, SARS, and MERS as positive controls, with a concentration of 200,000 copies/ μ L
123 (Integrated DNA Technologies, IA, USA).



124

125 **Figure 1. Experimental setup.** (A) Commercial 200 microliter Eppendorf PCR tubes, and
126 (B) a 3D-printed incubator were used in amplification experiments of samples containing
127 synthetic SARS-CoV-2 nucleic acid material. (C) 3D CAD model of the LAMP reaction
128 incubator. (D) Actual image of the Eppendorf tube incubator connected to a conventional
129 water circulator.

130 Samples containing different concentrations of synthetic nucleic acids of SARS-CoV-2
131 were prepared by successive dilutions from stocks (from 2×10^5 copies to 65 copies). We
132 used a plasmid that contained the gene GP from EBOV as a negative control. The
133 production of this EBOV genetic material has been documented elsewhere by our group
134 [23].

135 *Amplification mix:* We used WarmStart® Colorimetric LAMP 2× Master Mix (DNA &
136 RNA) from New England Biolabs (MA, USA), and followed the recommended protocol:
137 12.5 µL Readymix, 1.6 µM FIP primer, 1.6 µM BIP primer, 0.2 µM F3 primer, 0.2 µM B3
138 primer, 0.4 µM LF primer, 0.4 µM LB primer, 1µL DNA template (~ 625 to 2×10^5 DNA
139 copies), 1.25 µL EvaGreen® Dye from Biotium (CA, USA), and nuclease-free water to a
140 final volume of reaction 25 µL. This commercial mix contains phenol red as a pH indicator
141 for revealing the shift of pH during LAMP amplification across the threshold of pH=6.8.

142

143 *Primers used:* Two different sets of LAMP primers, referred to here as α and β , were
144 designed in house using the LAMP primer design software Primer Explorer V5
145 (<http://primerexplorer.jp/lampv5e/index.html>). These primers were based on the analysis of
146 alignments of the SARS-Co2 N gene sequences using the software Geneious (New
147 Zealand), downloaded from [https://www.ncbi.nlm.nih.gov/genbank/sars-cov-2-](https://www.ncbi.nlm.nih.gov/genbank/sars-cov-2-seqs/#nucleotide-sequences)
148 [seqs/#nucleotide-sequences](https://www.ncbi.nlm.nih.gov/genbank/sars-cov-2-seqs/#nucleotide-sequences).

149 Each set, containing six LAMP primers, were used to target two different regions of the
150 sequence of the SARS-Co2 N gene. In addition, for comparison purposes, we conducted
151 PCR amplification experiments using the primer sets recommended by the CDC for the
152 standard diagnostics of COVID-19 (i.e., N1, N2, and N3 assays) using RT-qPCR. The

153 sequences of our LAMP primers are presented in Table 1. The sequences of the PCR
 154 primers (N1–N3) have been reported elsewhere[24,46].

155

156 *Amplification protocols:* For all LAMP experiments, we performed isothermal heating for
 157 30 or 60 min. In our experiments, we tested three different temperatures: 50, 60, and 65 °C.

158 **Table 1. Primer sequences used in LAMP amplification experiments.** Two different sets of
 159 primers were used, directed at the RNA sequence encoding the N sequence of the SARS-CoV-2.

Set	Description	Primers Sequence (5'>3')
<i>Primer set α</i>	2019-nCoV 1-F3	TGGACCCCAAAATCAGCG
	2019-nCoV 1-B3	GCCTTGTCCTCGAGGGAAT
	2019-nCoV 1-FIP	CCACTGCGTTCTCCATTCTGGTAAATGCACCCCGCATTACG
	2019-nCoV 1-BIP	CGCGATCAAACAACGTCGGCCCTTGCCATGTTGAGTGAGA
	2019-nCoV 1-LF	TGAATCTGAGGGTCCACCAA
	2019-nCoV 1-LB	TTACCCAATAATACTGCGTCTTGGT
<i>Primer set β</i>	2019-nCoV 2-F3	CCAGAATGGAGAACGCAGTG
	2019-nCoV 2-B3	CCGTCACCACCACGAATT
	2019-nCoV 2-FIP	AGCGGTGAACCAAGACGCAGGGCGCGATCAAACAACG
	2019-nCoV 2-BIP	AATTCCCTCGAGGACAAGGCGAGCTCTTCGGTAGTAGCCAA
	2019-nCoV 2-LF	TTATTGGGTAAACCTTGGGGC
	2019-nCoV 2-LB	TAACACCAATAGCAGTCCAGATGA

160

161 *Documentation of LAMP products:* We analyzed 10 μL of each LAMP reaction in a
 162 blueGel unit, a portable electrophoresis unit sold by MiniPCR from Amplyus (MA, USA).
 163 This is a compact electrophoresis unit (23 × 10 × 7 cm) that weighs 350 g. In these
 164 experiments, we analyzed 10 μL of the LAMP product using 1.2 % agarose electrophoresis

165 tris-borate-EDTA buffer (TBE). We used the Quick-Load Purple 2-Log DNA Ladder
166 (NEB, MA, USA) as a molecular weight marker. Gels were dyed with Gel-Green from
167 Biotium (CA, USA) using a 1:10,000 dilution, and a current of 48 V was supplied by the
168 blueGel built-in power supply (AC 100–240V, 50–60Hz).

169 As an alternative method for detection and reading of the amplification product, we
170 evaluated the amplification products by detecting the fluorescence emitted by a DNA-
171 intercalating agent, the EvaGreen® Dye from Biotium (CA, USA), in a Synergy HT
172 microplate reader (BioTek Instruments, VT, USA). Briefly, 25 μ L of the LAMP reaction
173 was placed in separate wells of a 96-well plate following completion of the LAMP
174 incubation. A 125 μ L volume of nuclease-free water was added to each well for a final
175 sample volume of 150 μ L and the samples were well-mixed by pipetting. These
176 experiments were run in triplicate. The following conditions were used in the microplate
177 reader: excitation of 485/20, emission of 528/20, gain of 75. Fluorescence readings were
178 done from the top at room temperature.

179

180 *Color determination by image analysis:* We also photographically documented and
181 analyzed the progression of color changes in the positive and negative SARS-CoV-2
182 synthetic samples during the LAMP reaction time (i.e., from 0 to 50 min). For that purpose,
183 Eppendorf PCR tubes containing LAMP samples were photographed using a smartphone
184 (iPhone, from Apple, USA). We used an application for IOS (Color Companion, freely
185 available at Apple store) to determine the components of color of each LAMP sample in the
186 CIELab color space. Color differences between the positive samples and negative controls
187 were calculated as distances in the CIELab coordinate system according to the following
188 formula:

189 Color Distance_{sample-negative} = SQRT [(L_{sample}-L_{negative})² + (a_{sample}-a_{negative})² + (b_{sample}-b_{negative})²]

190

191 Here L, a, and b are the color components of the sample or the negative control in the

192 CIELab color space (Supplementary Figure 4).

193

194 **Results and Discussion**

195

196 **Rationale**

197 We have developed a simple diagnostic method for the detection of SARS-CoV-2, the

198 causal agent of COVID-19. The rationale underlying this strategy is centered on achieving

199 the simplest possible integration of easily available reagents, materials, and fabrication

200 techniques to facilitate fast and massive implementation during the current COVID-19

201 pandemics in low- or middle-income regions.

202 This method is based on the amplification of the genetic material of SARS-CoV-2 using a

203 loop-mediated isothermal amplification (LAMP). The amplification is conducted using a

204 commercial reaction mix in commercial and widely available 200 μ L Eppendorf PCR

205 tubes. Moreover, we have designed and fabricated a simple 3D-printed chamber (Figure 1)

206 for incubation of the Eppendorf tubes and to enable LAMP at high temperatures (50–65 °C)

207 and extended times (up to 1 h). We show that this incubation chamber, when connected to a

208 conventional water recirculator, enables the successful amplification of positive samples

209 (i.e., samples containing SARS-CoV-2 nucleic acids).

210 This incubation chamber is one of the key elements that enable rapid and widespread

211 implementation of this diagnostic method at low cost. This 3D-printed incubator can be

212 rapidly printed using standard SLA printers widely available in markets worldwide.

213 Standard 3D-printing resins can be used. The availability of the original AutoCAD files
214 (included here as supplemental material) enables fast modification/optimization of the
215 design for accommodation of a larger number of samples or larger or smaller tubes,
216 adaptation to any available hoses (tubing), and possible incorporation of an on-line color
217 reading system. Indeed, all this is consistent with the main rationale of our proposed
218 diagnostic strategy for pandemic COVID-19: To enabling a fast and feasible response using
219 widespread, distributed, and scalable diagnostics fabricated with widely available
220 resources.

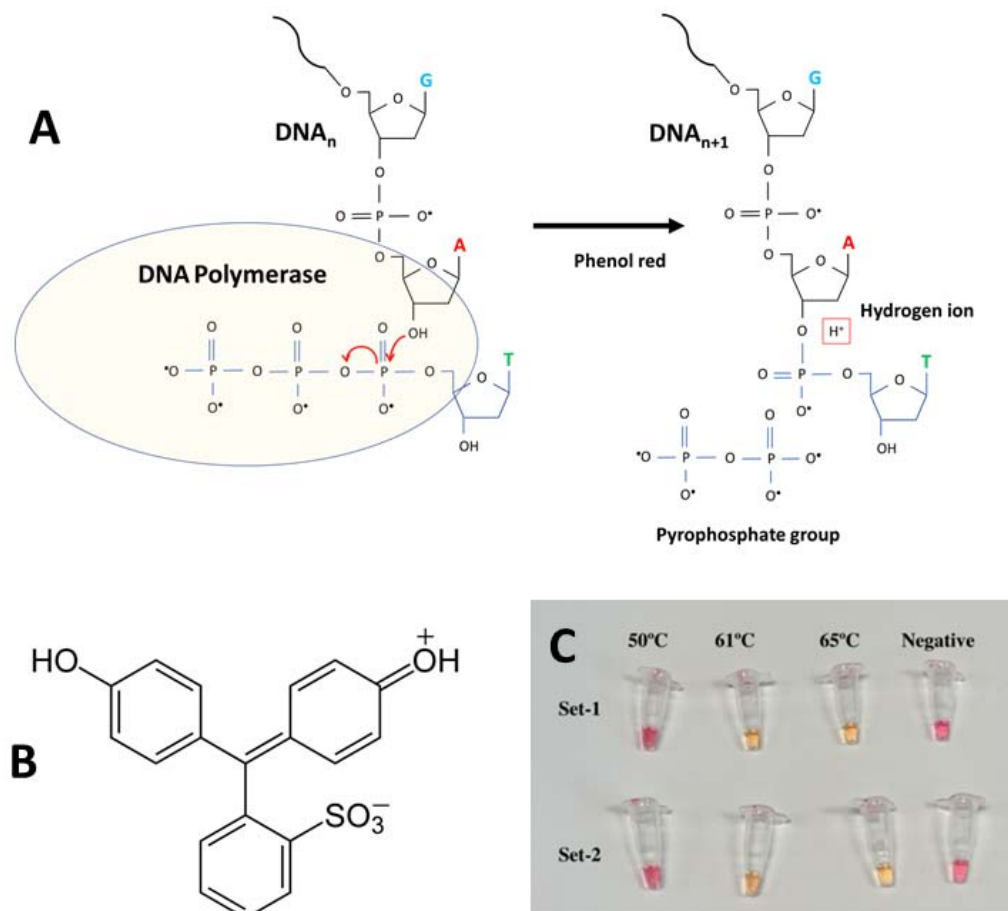
221 In the following section, we briefly discuss the mechanisms of amplification and visual
222 discrimination between positive and negative samples.

223

224 **Colorimetric LAMP amplification**

225 The presence of phenol red within the LAMP reaction mix allows for naked-eye
226 discrimination between positive and negative samples. The reaction mix is coupled with the
227 pH color transition of phenol red, a widely used pH indicator, which shifts in color from red
228 to yellow at pH 6.8. During LAMP amplification, the pH of the reaction mix continuously
229 evolves from neutrality to acidic values as protons are produced [27,47]. The mechanism of
230 production of hydrogen ions (H^+) during amplification in weakly buffered solutions has
231 been described [47]. DNA polymerases incorporate a deoxynucleoside triphosphate into the
232 nascent DNA chain. During this chemical event, a pyrophosphate moiety and a hydrogen
233 ion are released as byproducts (Figure 2 A). This release of hydrogen ions is quantitative,
234 according to the reaction scheme illustrated in Figure 2. The caudal of H^+ is high, since it is
235 quantitatively proportional to the number of newly integrated dNTPs. In fact, the

236 quantitative production of H^+ is the basis of previously reported detection methods, such as
237 the semiconductor sequencing technology operating in Ion Torrent sequencers[48].



238

239 **Figure 2. Initiators and pH indicator for SARS-Co2 detection using a colorimetric**
240 **LAMP method.** (A) LAMP reaction scheme. (B) Chemical structure of phenol red. (C)
241 Two different sets of LAMP primers were used for successfully targeting a gene sequence
242 encoding the SARS-Co2 N protein. Successful targeting and amplification is clearly
243 evident to the naked eye: positive samples shift from red to yellow.

244

245 In the initially neutral and weakly buffered reaction mixes, the production of H^+ during
246 LAMP amplification progressively and rapidly shifts the pH across the threshold of phenol
247 red (Figure 2B).

248 Moreover, the pH shift is clearly evident to the naked eye, thereby freeing the user from
249 reliance on spectrophotometric instruments and facilitating simple implementation during
250 emergencies (Figure 2C). Images in Figure 2C show representative colors of the
251 amplification reaction mixes contained in Eppendorf PCR tubes after incubation for 30
252 min. Three different incubation temperatures were tested (50, 60, and 65 °C) and two
253 different sets of LAMP-primers (α and β) were used.

254 Both sets of primers performed equivalently, at least based on visual inspection, in the three
255 temperature conditions tested. Discrimination between positive and negative controls is
256 possible using only the naked eye to discern the reaction products from amplifications
257 conducted at 60 and 65 °C. No or negligible amplification was evident at 50 °C or in the
258 control group.

259 Furthermore, we were able to successfully discriminate between positive and negative
260 samples using LAMP reaction mix already added with primers and kept at room
261 temperature for 48 h or at 4 °C for 72 hours (Figure S3). The stability of the reaction, the
262 isothermal nature of the amplification process, and its independence from specialized
263 equipment greatly simplifies the logistic of implementation of this diagnostic method
264 outside centralized labs.

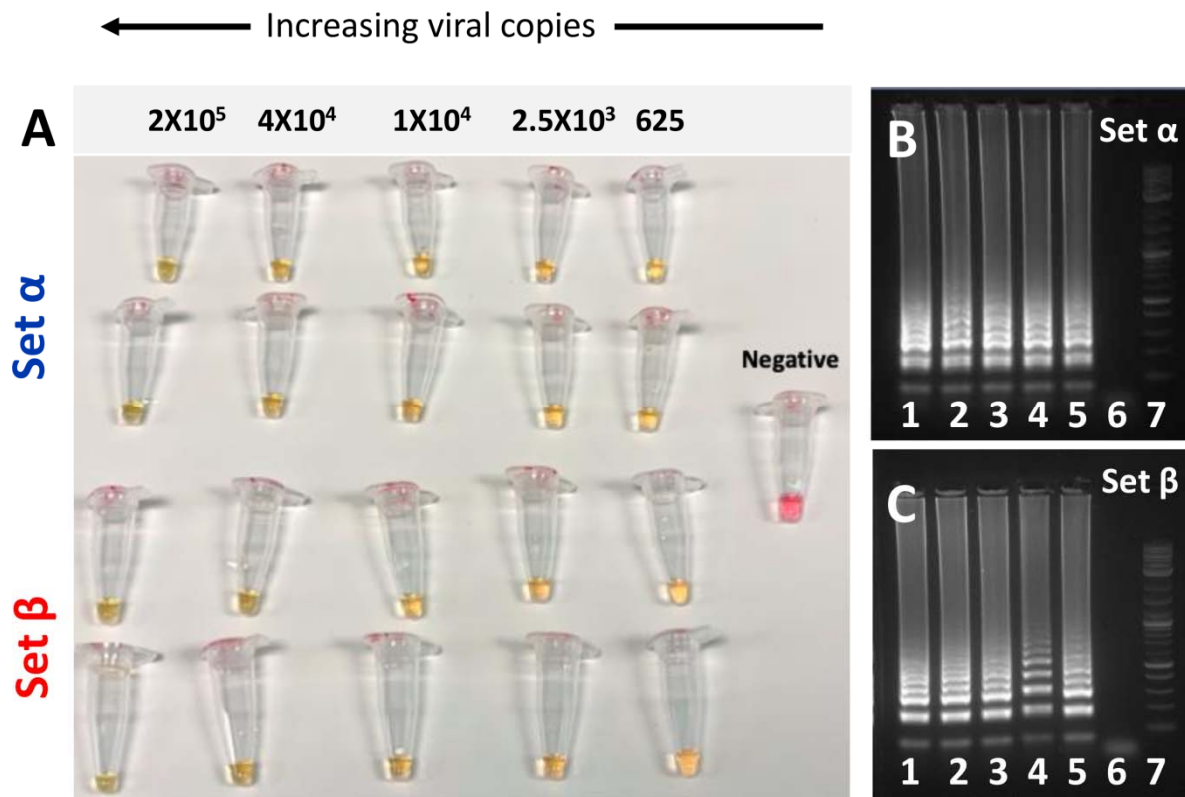
265

266 **Analysis of sensitivity**

267 We conducted a series of experiments to assess the sensitivity of the LAMP reactions in the
268 3D-printed incubation chamber using the two sets of primers (α and β ; Table 1). The
269 amplification proceeds with sufficient quality to also allow proper visualization of the
270 amplification products in electrophoresis gels, even at low nucleic acid concentrations. We
271 observed that amplification proceeded successfully in a wide range of viral loads, from 625

272 to 5×10^5 copies in experiments using synthetic SARS-CoV-2 nucleic acid material (Figure
273 3A).

274



275

276 **Figure 3. Two different sets of LAMP-primers were used for successfully targeting of**
277 **a gene sequence encoding the SARS-Co2 N protein.** (A) LAMP primer sets α and β both
278 enable the amplification of synthetic samples of SARS-CoV-2 nucleic acids in a wide range
279 of template concentrations, from 625 to 2.0×10^5 DNA copies of SARS-CoV-2 when
280 incubated for 50 minutes at a temperature range from 60 to 65 °C. (B,C) Agarose gel
281 electrophoresis of DNA amplification products generated by targeting two different regions
282 of the sequence coding for SARS-Co2 N protein. Two different primer sets were used: (B)
283 primer set α , and (C) primer set β . The initial template amount was gradually decreased
284 from left to right: 2.0×10^5 DNA copies (lane 1), 4.0×10^4 copies, (lane 2), 1.0×10^4 copies
285 (lane 3), 2.5×10^3 copies (lane 4), 625 copies (lane 5), negative control (lane 6), and
286 molecular weight ladder (lane 7).

287

288 We clearly observed amplification in samples containing as few as 625 viral copies after
289 incubation times of 5 min at 65 °C. If we put this range into a proper clinical context, the
290 actual viral load of COVID-19 in nasal swabs from patients has been estimated to fall
291 within the range of 10^5 to 10^6 viral copies per mL [49]. Discrimination between positive
292 and negative samples (controls) can be clearly established by the naked eye in all reactions
293 incubated for 50 min, regardless of the number of viral copies present. In addition, we did
294 not observe any non-specific amplification in negative samples (i.e., containing synthetic
295 genetic material from EBOV) incubated for 50 min at 65 °C. Indeed, the identification and
296 amplification of SARS-CoV-2 synthetic material is feasible in samples that contained ~62.5
297 viral copies using this LAMP strategy (Figure S3) and incubation times of 50–60 min.

298 We corroborated the amplification by visualizing LAMP products with gel electrophoresis
299 for the different viral loads tested. Figures 3B,C show agarose gels of the amplification
300 products of each one of the LAMP experiments, where two different sets of primers (α and
301 β) were used to amplify the same range of concentrations of template (from 625 to 2×10^5
302 synthetic viral copies). We were able to generate a visible array of bands of amplification
303 products, a typical signature of LAMP, for both LAMP primer sets and across the whole
304 range of synthetic viral loads. Indeed, both primer sets rendered similar amplification
305 profiles.

306 In summary, using the primers and methods described here, we were able to consistently
307 detect the presence of SARS-CoV-2 synthetic nucleic acids. We have used a simple 3D-
308 printed incubator, connected to a water circulator, to conduct LAMP. We show that, after
309 only 30 min of incubation, samples containing a viral load in the range of 10^4 to 10^5 copies
310 could be clearly discriminated from negative samples by visual inspection with the naked
311 eye (Figure 2C). Samples with a lower viral load were clearly discriminated when the

312 LAMP reaction was incubated for 50 min. Incubation periods of up to 1 h at 68 °C did not
313 induced false positives and were able to amplify as few as ~62 copies of SARS-CoV-2
314 synthetic genetic material. These results are consistent with those of other reports in which
315 colorimetric LAMP, assisted by phenol red, has been used to amplify SARS-COV-2
316 genetic material [39,40].

317 We observe 0 false positive cases in experiments where synthetic samples containing
318 EBOV genetic material were incubated at 65 °C for 1 h.

319 In the current context of the COVID-19 pandemics, the importance of communicating this
320 result does not reside in its novelty but in its practicality. Some cost considerations follow.

321 While the market value of a traditional RT-qPCR apparatus (the current gold standard for
322 COVID-19 diagnostics) is in the range of 10,000 to 40,000 USD, a 3D-printed incubator,
323 such as the one described here (Figure S1,S2; Supplementary file S1), could be fabricated
324 for under 200 USD at any 3D printer shop. This difference is significant, especially during
325 an epidemic or pandemic crisis when rational investment of resources is critical. While the
326 quantitative capabilities of testing using an RT-qPCR platform are undisputable, the
327 capacity of many countries to rapidly, effectively, and massively establish diagnostic
328 centers based on RT-qPCR is questionable. The current pandemic scenarios experienced in
329 the USA, Italy, France, and Spain, among others, have crudely demonstrated that
330 centralized labs are not an ideal solution during emergencies. Portable diagnostic systems
331 may provide a vital flexibility and speed of response that RT-qPCR platforms cannot
332 deliver.

333

334

335

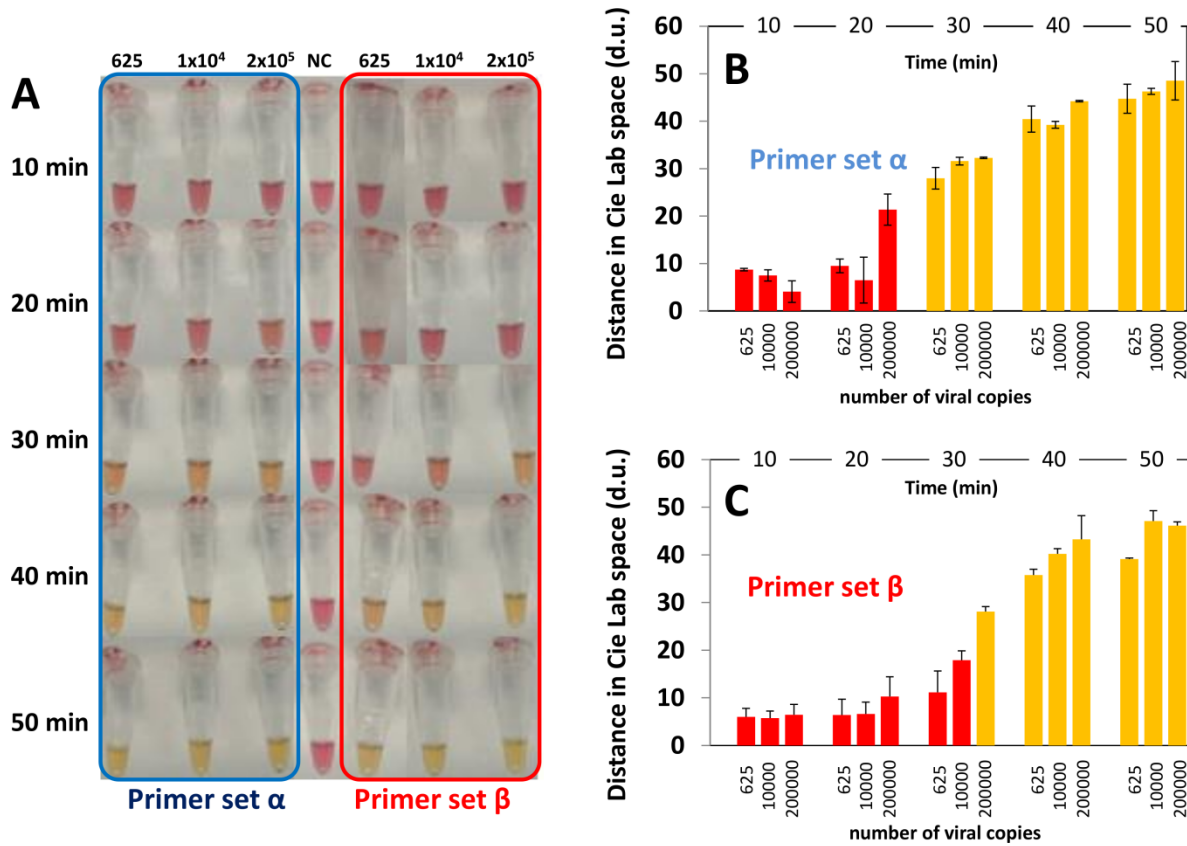
336 **Feasibility of real-time quantification**

337 Here, we further illustrate the deterministic and quantitative dependence between the
338 concentration of the amplification product and the color signal produced during this
339 colorimetric LAMP reaction. For this purpose, we simulated real-time amplification
340 experiments by conducting a series of amplification reactions using initial amounts of 625,
341 1×10^4 , and 2×10^5 copies of synthetic SARS-CoV-2 genetic material in our 3D-printed
342 incubator.

343 We extracted samples from the incubator after 0, 10, 20, 30, 40, and 50 min of incubation at
344 65 °C. The color of these samples was documented as images captured using a smart phone
345 (iPhone 7) against a white background (Figure 4A). The images were analyzed using the
346 free access application Color Companion® for the iPhone or iPad. Briefly, color images
347 were decomposed into their CIELab space components. In the CIELab color space, each
348 color can be represented as a point in a 3D-space, defined by the values **L**, **a**, and **b** [45]. In
349 this coordinate system, **L** is the luminosity (which ranges from 0 to +100), **a** is the blue-
350 yellow axis (which ranges from -50 to 50), and **b** is the green-red axis (which ranges from -
351 50 to 50) (Figure S4).

352 The difference between two colors can be quantitatively represented as the distance
353 between the two points that those colors represent in the CIELab coordinate system. For the
354 colorimetric LAMP reaction mixture used in our experiments, the spectrum of possible
355 colors evolves from red (for negative controls and negative samples) to yellow (for positive
356 samples). Conveniently, the full range of colors for samples and controls can be represented
357 in the red and yellow quadrant defined by **L** [0,50], **a** [0,50], and **b** [0,50]. For instance, the
358 difference between the color of a sample (at any time of the reaction) and the color of the

359 negative control (red; $L=53.72 \pm 0.581$, $a=38.86 \pm 2.916$, and $b=11.86 \pm 0.961$) can be
 360 calculated in the CIELab space.



361

362 **Figure 4.** Evaluation of the sensitivity of the combined use of a colorimetric LAMP method
 363 assisted by the use of phenol red. (A) Sensitivity trials using different concentrations of the template
 364 (positive control) and two different primers sets: α (indicated in blue) and β (indicated in red).
 365 Photographs of the Eppendorf PCR tubes containing positive samples and negative controls were
 366 acquired using a smartphone. (C,D) Distance in the color CIELab space between negative controls
 367 (red) and samples containing different concentrations of SARS-CoV-2 nucleic acid material (i.e.,
 368 625, 10000, and 200000 synthetic copies) analyzed after different times of incubation (i.e., 10, 20,
 369 30, 40, and 50 minutes) at 65 °C. The analysis of color distances is presented for amplifications
 370 conducted using primer set (B) α and (C) β .

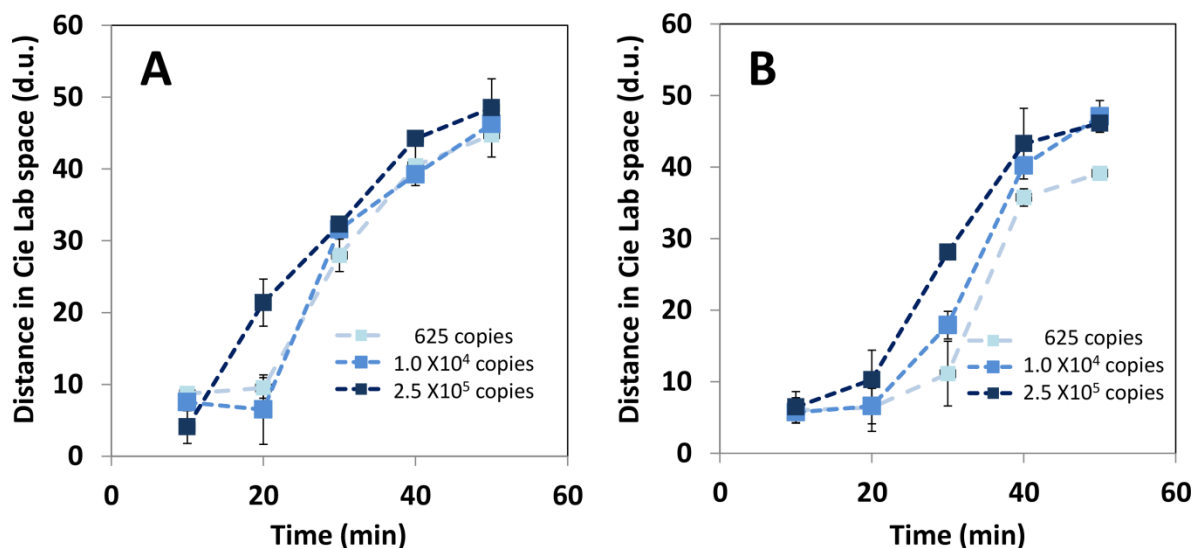
371

372 We determined the distance in the CIELab space between the color of samples taken at
 373 different incubation times that contained SARS-CoV-2 genetic material and negative

374 controls (Figure 4B and C). We repeated this calculation for each of the LAMP primer sets
375 that we used, namely primer set α (Figure 4B) and β (Figure 4C).
376 These results suggest that the color difference between the samples and negative controls is
377 quantifiable. Therefore, color analysis may be implemented to assist the discrimination
378 between positives and negatives. Furthermore, imaging and color analysis techniques may
379 be implemented in this simple colorimetric LAMP diagnostic strategy to render a real-time
380 quantitative Lamp (RT-qLAMP). Alternatively, the progression of the amplification at
381 different times can be monitored by adding an intercalating DNA agent, (i.e., EvaGreen
382 Dye), and measuring fluorescence on time (Figure S5).
383 Note that the variance coefficients for the control are 1.08, 7.50, and 8.10% for L, a, and b,
384 respectively. These small values suggest robustness and reproducibility in the location of
385 the coordinates of the control point (reference point). Similarly, the variation in color
386 between negative controls and positive samples incubated for 50 min was reproducible and
387 robust (average of 46.60 +/- 4.02 d.u.; variance coefficient of 8.62%).
388 Finally, we observed differences in the performance of the two LAMP primer sets used in
389 the experiments reported here (Figure 4B and 5).
390 Our results suggest that primer set α enabled faster amplification in samples with fewer
391 viral copies. Consistently, this primer set yielded positive discrimination in samples with
392 625 viral copies in 30 min (Figure 4B). The use of primer set β enabled similar differences
393 in color, measured as distances in the CIELAB 3D-space, in 40 min (Figure 4C). These
394 findings suggest that primer set α should be preferred for final-point implementations of
395 this colorimetric LAMP method. Interestingly, primer set β may better serve the purpose of
396 a real-time implementation. While primer set α produced similar trajectories of evolution of
397 color in samples that contained 1.0×10^4 and 2.0×10^5 viral copies (Figure 5A), primer set

398 β was better at discriminating between amplifications produced from different initial viral
399 loads (Figure 5B).

400



401

402 **Figure 5.** Time progression of the distance in color with respect to negative controls (red
403 color) in the CIE Lab space for positive SARS-CoV-2 samples containing 625 (light blue,
404 \blacksquare), 1×10^4 (medium blue, \blacksquare), and 2.5×10^6 (dark blue, \blacksquare) copies of synthetic of SARS-
405 CoV-2 nucleic acids. Results obtained in experiments using (A) primer set α , and (B)
406 primer set β .

407

408 Conclusions

409 The challenge of point-of-care detection of viral threats is of paramount importance,
410 particularly in underdeveloped regions and in emergency situations (i.e., epidemic
411 outbreaks). In the context of the current COVID-19 pandemic, the availability of testing
412 infrastructure based on RT-qPCR is recognized as a serious challenge around the world. In
413 developing economies (i.e. Latin America, India, and most African countries), the currently
414 available resources for massive COVID-19 testing by RT-qPCR will clearly be insufficient.

415 Even in developed countries, the time to get diagnostic RT-qPCR results from a COVID-19
416 RT-qPCR test currently ranges from 1 to 5 days. Clearly, the available PCR labs are
417 overburdened with samples, have too few personnel to conduct the tests, are struggling with
418 backlogs on the instrumentation, and face complicated logistics to transport delicate and
419 infective samples while preserving the cold chain.

420 Here, we have demonstrated that a simple embodiment of a LAMP reaction, assisted by the
421 use of phenol red as a pH indicator and the use of a simple 3D-printed chamber connected
422 to a water circulator, can enable the rapid and highly accurate identification of samples that
423 contain artificial SARS-CoV-2 genetic sequences. Amplification is visually evident,
424 without the need for any additional instrumentation, even at low viral copy numbers. In our
425 experiments with synthetic samples, we observed 100 percent accuracy in samples
426 containing as few as 625 copies of SARS-CoV-2 genetic material.

427 Validation of these results using real human samples from positive and negative COVID-19
428 subjects is obviously needed to obtain a full assessment of the potential of this strategy as
429 an alternative to RT-qPCR platforms. However, our results with synthetic samples suggest
430 that this simple strategy may greatly enhance the capabilities for COVID-19 testing in
431 situations where RT-qPCR is not feasible or is unavailable.

432

433 **Acknowledgments**

434 EGG acknowledges funding from a doctoral scholarship provided by CONACyT (Consejo
435 Nacional de Ciencia y Tecnología, México). GTdS and MMA acknowledge the
436 institutional funding received from Tecnológico de Monterrey (Grant 002EICIS01), and
437 funding provided by CONACyT (Consejo Nacional de Ciencia y Tecnología, México)
438 through grants (SNI 26048, SNI 256730, and Scholarships 635891, 856068, and 814593).

439 **Supporting Information**

440 **Supporting Information**

441 **Figure S1.** (A) Actual images, and (B) rendering of the 3D- printed incubation chamber
442 used in the LAMP experiments.

443

444 **Figure S2.** Schematic representation of the chamber (different views) showing its relevant
445 dimensions.

446

447 **Figure S3.** (A) The colorimetric LAMP method described here was able to identify and
448 amplify synthetic SARS-CoV-2 genetic material in samples containing as few as ~62 viral
449 copies. (B) Evaluation of the stability and functionality of the LAMP reaction mix at
450 different storage times and temperatures. The reaction mix, which is formulated with
451 LAMP primers and ready for the addition of nucleic acid extracts, is functional and
452 discriminates between positive and negative samples when stored (i) at room temperature
453 for 48 h or (ii) at 4 °C for 72 h.

454

455 **Figure S4.** (A) Color analysis conducted on positive and negative SARS-CoV-2 samples
456 contained in Eppendorf PCR tubes (yellow inset) using Color Companion, a freely
457 available app from Apple (downloadable at Apple Store, USA). This app identifies the
458 components of color in a specific location of an image (black circle in the yellow inset) in
459 the CIELab, RGB, HSB, or CMYK spaces. The image can be uploaded using e-mail,
460 airdrop, or Whatsapp. (B) Schematic representation of the CIELab space, a color system
461 where any color can be represented in terms of a point and its coordinates in a 3D space,
462 where L is luminosity, a is the axis between green and red, and b is the axis between yellow
463 and red.

464

465 **Figure S5.** (A) The amount of amplification product in LAMP experiments was evaluated
466 by measuring the fluorescence emitted by the amplification product in reactions with an
467 added intercalating agent. Fluorescence readings were conducted in standard 96-well plates
468 and using a conventional plate reader. (A) Fluorescence readings, as measured in a

469 commercial plate reader, for different dilutions of SARS-CoV-2 synthetic DNA templates.
470 Results using two different LAMP primer sets are shown: set α (indicated in blue), and set
471 β (indicated in red).

472

473

474 **References**

- 475 1. Coronavirus Disease (COVID-19) – Statistics and Research - Our World in Data
476 [Internet]. [cited 8 Apr 2020]. Available:
477 [https://ourworldindata.org/coronavirus?fbclid=IwAR28tcRVA1rmXsVcRYHcxuHp](https://ourworldindata.org/coronavirus?fbclid=IwAR28tcRVA1rmXsVcRYHcxuHpRXKeyO9-uxFJFSG5-lv5gsJgzDxK7eN08i_Y)
478 [RXKeyO9-uxFJFSG5-lv5gsJgzDxK7eN08i_Y](https://ourworldindata.org/coronavirus?fbclid=IwAR28tcRVA1rmXsVcRYHcxuHpRXKeyO9-uxFJFSG5-lv5gsJgzDxK7eN08i_Y)
- 479 2. Bedford J, Enria D, Giesecke J, Heymann DL, Ihekweazu C, Kobinger G, et al.
480 COVID-19: towards controlling of a pandemic. *The Lancet*. Lancet Publishing
481 Group; 2020. pp. 1015–1018. doi:10.1016/S0140-6736(20)30673-5
- 482 3. Cohen J, Kupferschmidt K. Countries test tactics in “war” against COVID-19.
483 *Science*. American Association for the Advancement of Science; 2020;367: 1287–
484 1288. doi:10.1126/science.367.6484.1287
- 485 4. Pung R, Chiew CJ, Young BE, Chin S, I-C Chen M, Clapham HE, et al. Articles
486 Investigation of three clusters of COVID-19 in Singapore: implications for
487 surveillance and response measures. *Lancet*. Elsevier; 2020;19: 1–8.
488 doi:10.1016/S0140-6736(20)30528-6
- 489 5. Alvarez MM, Gonzalez-Gonzalez E, Santiago GT. Modeling COVID-19 epidemics
490 in an Excel spreadsheet: Democratizing the access to first-hand accurate predictions
491 of epidemic outbreaks. medRxiv. Cold Spring Harbor Laboratory Press; 2020;
492 2020.03.23.20041590. doi:10.1101/2020.03.23.20041590
- 493 6. Singh R, Adhikari R. Age-structured impact of social distancing on the COVID-19

- 494 epidemic in India. 2020; Available: <http://arxiv.org/abs/2003.12055>
- 495 7. Bastos SB, Cajueiro DO. Modeling and forecasting the Covid-19 pandemic in
496 Brazil. 2020; Available: <http://arxiv.org/abs/2003.14288>
- 497 8. Yen C-W, de Puig H, Tam JO, Gómez-Márquez J, Bosch I, Hamad-Schifferli K, et
498 al. Multicolored silver nanoparticles for multiplexed disease diagnostics:
499 distinguishing dengue, yellow fever, and Ebola viruses. *Lab Chip. The Royal Society*
500 *of Chemistry*; 2015;15: 1638–1641. doi:10.1039/C5LC00055F
- 501 9. Mou L, Jiang X. Materials for Microfluidic Immunoassays: A Review. *Adv Healthc*
502 *Mater. Wiley-VCH Verlag*; 2017;6: 1601403. doi:10.1002/adhm.201601403
- 503 10. Alvarez MM, López-Pacheco F, Aguilar-Yañez JM, Portillo-Lara R, Mendoza-
504 Ochoa GI, García-Echauri S, et al. Specific Recognition of Influenza A/H1N1/2009
505 Antibodies in Human Serum: A Simple Virus-Free ELISA Method. Jeyaseelan S,
506 editor. *PLoS One. Public Library of Science*; 2010;5: e10176.
507 doi:10.1371/journal.pone.0010176
- 508 11. Zhong L, Chuan J, Gong B, Shuai P, Zhou Y, Zhang Y, et al. Detection of serum
509 IgM and IgG for COVID-19 diagnosis. *Sci CHINA Life Sci. Science China Press*;
510 2020; doi:10.1007/S11427-020-1688-9
- 511 12. Pardee K, Green AA, Takahashi MK, Braff D, Lambert G, Lee JW, et al. Rapid,
512 Low-Cost Detection of Zika Virus Using Programmable Biomolecular Components.
513 *Cell. Cell Press*; 2016;165: 1255–1266. doi:10.1016/J.CELL.2016.04.059
- 514 13. Broughton JP, Deng X, Yu G, Fasching CL, Streithorst J, Granados A, et al. Rapid
515 Detection of 2019 Novel Coronavirus SARS-CoV-2 Using a CRISPR-based 1
516 DETECTR Lateral Flow Assay 2 3. doi:10.1101/2020.03.06.20032334
- 517 14. Chen JS, Ma E, Harrington LB, Da Costa M, Tian X, Palefsky JM, et al. CRISPR-

- 518 Cas12a target binding unleashes indiscriminate single-stranded DNase activity.
519 Science (80-). American Association for the Advancement of Science; 2018;360:
520 436–439. doi:10.1126/science.aar6245
- 521 15. Elizondo-Montemayor L, Alvarez MM, Hernández-Torre M, Ugalde-Casas PA,
522 Lam-Franco L, Bustamante-Careaga H, et al. Seroprevalence of antibodies to
523 influenza A/H1N1/2009 among transmission risk groups after the second wave in
524 Mexico, by a virus-free ELISA method. *Int J Infect Dis.* Elsevier; 2011;15: e781–
525 e786. doi:10.1016/j.ijid.2011.07.002
- 526 16. Tang Y-W, Schmitz JE, Persing DH, Stratton CW. The Laboratory Diagnosis of
527 COVID-19 Infection: Current Issues and Challenges. *J Clin Microbiol.* American
528 Society for Microbiology Journals; 2020; doi:10.1128/JCM.00512-20
- 529 17. Wölfel R, Corman VM, Guggemos W, Seilmaier M, Zange S, Müller MA, et al.
530 Virological assessment of hospitalized patients with COVID-2019. *Nature.* Nature
531 Publishing Group; 2020; 1–10. doi:10.1038/s41586-020-2196-x
- 532 18. Mauk MG, Song J, Bau HH, Liu C. Point-of-Care Molecular Test for Zika Infection.
533 *Clin Lab Int.* NIH Public Access; 2017;41: 25–27. Available:
534 <http://www.ncbi.nlm.nih.gov/pubmed/28819345>
- 535 19. Liao S-C, Peng J, Mauk MG, Awasthi S, Song J, Friedman H, et al. Smart cup: A
536 minimally-instrumented, smartphone-based point-of-care molecular diagnostic
537 device. *Sensors Actuators B Chem.* Elsevier; 2016;229: 232–238.
538 doi:10.1016/J.SNB.2016.01.073
- 539 20. Jansen van Vuren P, Grobbelaar A, Storm N, Conteh O, Konneh K, Kamara A, et al.
540 Comparative Evaluation of the Diagnostic Performance of the Prototype Cepheid
541 GeneXpert Ebola Assay. *J Clin Microbiol.* American Society for Microbiology;

- 542 2016;54: 359–67. doi:10.1128/JCM.02724-15
- 543 21. Craw P, Balachandran W. Isothermal nucleic acid amplification technologies for
544 point-of-care diagnostics: a critical review. *Lab Chip. The Royal Society of*
545 *Chemistry*; 2012;12: 2469. doi:10.1039/c2lc40100b
- 546 22. Hsieh K, Patterson AS, Ferguson BS, Plaxco KW, Soh HT. Rapid, sensitive, and
547 quantitative detection of pathogenic DNA at the point of care through microfluidic
548 electrochemical quantitative loop-mediated isothermal amplification. *Angew Chem*
549 *Int Ed Engl. NIH Public Access*; 2012;51: 4896–900. doi:10.1002/anie.201109115
- 550 23. Gonzá Lez-Gonzá Lez E, Mendoza-Ramos JL, Pedrozaid SC, Cuellar-Monterrubio
551 A, Má Rquez-Ipiña AR, Lira-Serhanid D, et al. Validation of use of the miniPCR
552 thermocycler for Ebola and Zika virus detection. 2019;
553 doi:10.1371/journal.pone.0215642
- 554 24. Gonzalez-Gonzalez E, Santiago GT, Lara-Mayorga IM, Martinez-Chapa SO,
555 Alvarez MM. Portable and accurate diagnostics for COVID-19: Combined use of the
556 miniPCR thermocycler and a well-plate reader for SARS-Co2 virus detection.
557 medRxiv. Cold Spring Harbor Laboratory Press; 2020; 2020.04.03.20052860.
558 doi:10.1101/2020.04.03.20052860
- 559 25. Lan L, Xu D, Ye G, Xia C, Wang S, Li Y, et al. Positive RT-PCR Test Results in
560 Patients Recovered From COVID-19. *JAMA*. 2020; doi:10.1001/jama.2020.2783
- 561 26. El-Tholoth M, Bau HH, Song J. A Single and Two-Stage, Closed-Tube, Molecular
562 Test for the 2019 Novel Coronavirus (COVID-19) at Home, Clinic, and Points of
563 Entry. *ChemRxiv*; 2020; doi:10.26434/CHEMRXIV.11860137.V1
- 564 27. Kaarj K, Akarapipad P, Yoon JY. Simpler, Faster, and Sensitive Zika Virus Assay
565 Using Smartphone Detection of Loop-mediated Isothermal Amplification on Paper

- 566 Microfluidic Chips. *Sci Rep. Nature Publishing Group*; 2018;8: 1–11.
567 doi:10.1038/s41598-018-30797-9
- 568 28. Tomita N, Mori Y, Kanda H, Notomi T. Loop-mediated isothermal amplification
569 (LAMP) of gene sequences and simple visual detection of products. *Nat Protoc.*
570 *Nature Publishing Group*; 2008;3: 877–882. doi:10.1038/nprot.2008.57
- 571 29. Goto M, Honda E, Ogura A, Nomoto A, Hanaki KI. Colorimetric detection of loop-
572 mediated isothermal amplification reaction by using hydroxy naphthol blue.
573 *Biotechniques*. 2009;46: 167–172. doi:10.2144/000113072
- 574 30. Yang T, Wang Y-C, Shen C-F, Cheng C-M. Point-of-Care RNA-Based Diagnostic
575 Device for COVID-19. *Diagnostics. MDPI AG*; 2020;10: 165.
576 doi:10.3390/diagnostics10030165
- 577 31. Kozel TR, Burnham-Marusich AR. Point-of-Care Testing for Infectious Diseases:
578 Past, Present, and Future. *J Clin Microbiol. American Society for Microbiology*;
579 2017;55: 2313–2320. doi:10.1128/JCM.00476-17
- 580 32. Su W, Gao X, Jiang L, Qin J. Microfluidic platform towards point-of-care
581 diagnostics in infectious diseases. *J Chromatogr A. Elsevier*; 2015;1377: 13–26.
582 doi:10.1016/J.CHROMA.2014.12.041
- 583 33. Drancourt M, Michel-Lepage A, Boyer S, Raoult D. The Point-of-Care Laboratory
584 in Clinical Microbiology. *Clin Microbiol Rev. American Society for Microbiology*;
585 2016;29: 429–47. doi:10.1128/CMR.00090-15
- 586 34. Jangam SR, Agarwal AK, Sur K, Kelso DM. A point-of-care PCR test for HIV-1
587 detection in resource-limited settings. *Biosens Bioelectron. Elsevier*; 2013;42: 69–75.
588 doi:10.1016/J.BIOS.2012.10.024
- 589 35. Qiu X, Ge S, Gao P, Li K, Yang S, Zhang S, et al. A smartphone-based point-of-care

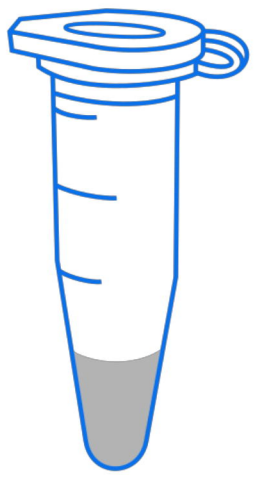
- 590 diagnosis of H1N1 with microfluidic convection PCR. *Microsyst Technol.* Springer
591 Berlin Heidelberg; 2017;23: 2951–2956. doi:10.1007/s00542-016-2979-z
- 592 36. Nguyen T, Duong Bang D, Wolff A. 2019 Novel Coronavirus Disease (COVID-19):
593 Paving the Road for Rapid Detection and Point-of-Care Diagnostics.
594 *Micromachines.* MDPI AG; 2020;11: 306. doi:10.3390/mi11030306
- 595 37. Udugama B, Kadhiresan P, Kozlowski HN, Malekjahani A, Osborne M, Li VYC, et
596 al. Diagnosing COVID-19: The Disease and Tools for Detection. *ACS Nano.*
597 American Chemical Society; 2020; doi:10.1021/acsnano.0c02624
- 598 38. Gates B. Responding to Covid-19 — A Once-in-a-Century Pandemic? *N Engl J*
599 *Med.* Massachusetts Medical Society; 2020; doi:10.1056/nejmp2003762
- 600 39. Yu L, Wu S, Hao X, Li X, Liu X, Ye S, et al. Rapid colorimetric detection of
601 COVID-19 coronavirus using a reverse tran-scriptional loop-mediated isothermal
602 amplification (RT-LAMP) diagnostic plat-form: iLACO. medRxiv. Cold Spring
603 Harbor Laboratory Press; 2020; 2020.02.20.20025874.
604 doi:10.1101/2020.02.20.20025874
- 605 40. Zhang Y, Odiwuor N, Xiong J, Sun L, Nyaruaba RO, Wei H, et al. Rapid Molecular
606 Detection of SARS-CoV-2 (COVID-19) Virus RNA Using Colorimetric LAMP.
607 medRxiv. Cold Spring Harbor Laboratory Press; 2020;2: 2020.02.26.20028373.
608 doi:10.1101/2020.02.26.20028373
- 609 41. Park G-S, Ku K, Beak S-H, Kim SJ, Kim S Il, Kim B-T, et al. Development of
610 Reverse Transcription Loop-mediated Isothermal Amplification (RT-LAMP) Assays
611 Targeting SARS-CoV-2. bioRxiv. Cold Spring Harbor Laboratory; 2020;
612 2020.03.09.983064. doi:10.1101/2020.03.09.983064
- 613 42. Zhu X, Wang X, Han L, Chen T, Wang L, Li H, et al. Reverse transcription loop-

- 614 mediated isothermal amplification combined with nanoparticles-based biosensor for
615 diagnosis of COVID-19. medRxiv. Cold Spring Harbor Laboratory Press; 2020;
616 2020.03.17.20037796. doi:10.1101/2020.03.17.20037796
- 617 43. Lamb LE, Bartolone SN, Ward E, Chancellor MB. Rapid Detection of Novel
618 Coronavirus (COVID19) by Reverse Transcription-Loop-Mediated Isothermal
619 Amplification. SSRN Electron J. Elsevier BV; 2020; doi:10.2139/ssrn.3539654
- 620 44. Jiang M, Fang W, Aratehfar A, Li X, ling L, Fang H, et al. Development and
621 validation of a rapid single-step reverse transcriptase loop-mediated isothermal
622 amplification (RT-LAMP) system potentially to be used for reliable and high-
623 throughput screening of COVID-19. medRxiv. Cold Spring Harbor Laboratory
624 Press; 2020; 2020.03.15.20036376. doi:10.1101/2020.03.15.20036376
- 625 45. Santiago GT De, Gante CR De, García-Lara S, Ballescá-Estrada A, Alvarez MM.
626 Studying mixing in Non-Newtonian blue maize flour suspensions using color
627 analysis. PLoS One. Public Library of Science; 2014;9.
628 doi:10.1371/journal.pone.0112954
- 629 46. OSF Preprints | Landscape Coronavirus Disease 2019 test (COVID-19 test) in vitro -
630 - A comparison of PCR vs Immunoassay vs Crispr-Based test [Internet]. [cited 8 Apr
631 2020]. Available: <https://osf.io/6eagn>
- 632 47. Tanner NA, Zhang Y, Evans TC. Visual detection of isothermal nucleic acid
633 amplification using pH-sensitive dyes. Biotechniques. Eaton Publishing Company;
634 2015;58: 59–68. doi:10.2144/000114253
- 635 48. Rusk N. Torrents of sequence. Nature Methods. Nature Publishing Group; 2011. p.
636 44. doi:10.1038/nmeth.f.330
- 637 49. Wang W, Xu Y, Gao R, Lu R, Han K, Wu G, et al. Detection of SARS-CoV-2 in

638 Different Types of Clinical Specimens. JAMA - Journal of the American Medical
639 Association. American Medical Association; 2020. doi:10.1001/jama.2020.3786
640
641
642
643
644

sample →

A

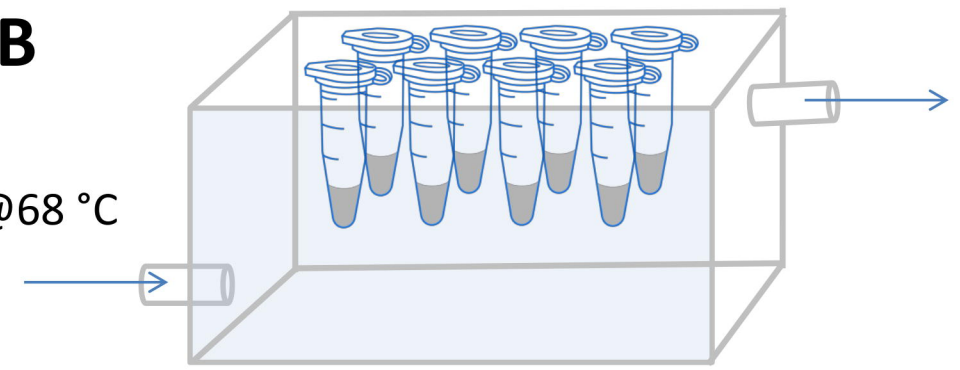


Reaction mix
+ Primer set α or β

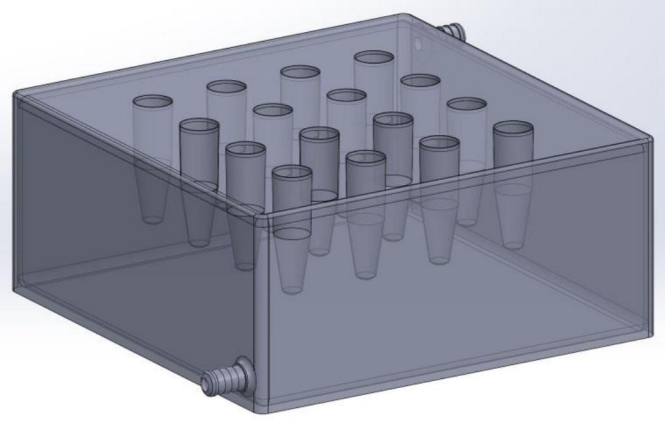
Polymerase
Phenol red

B

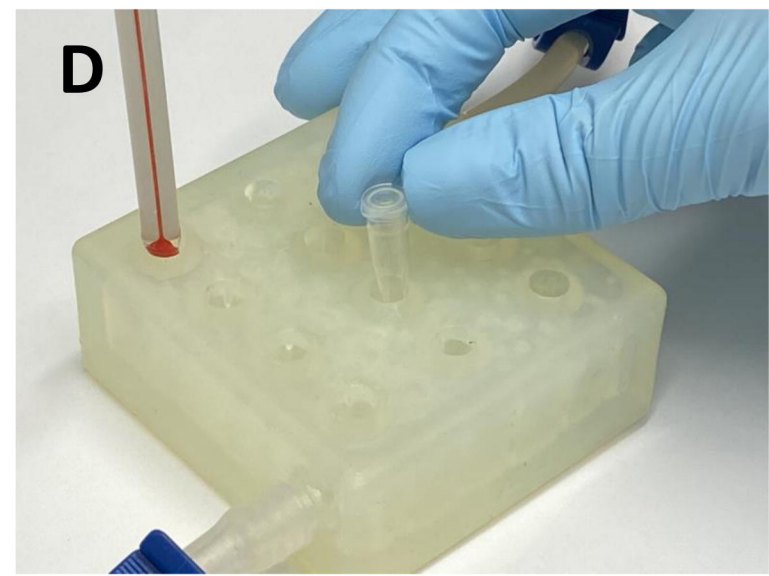
Water in @68 °C

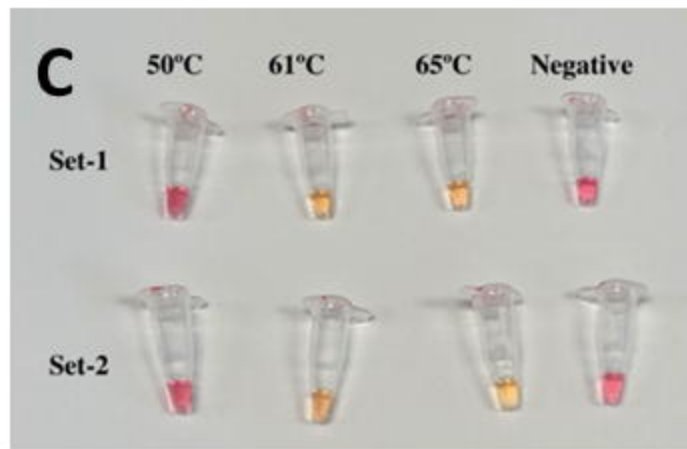
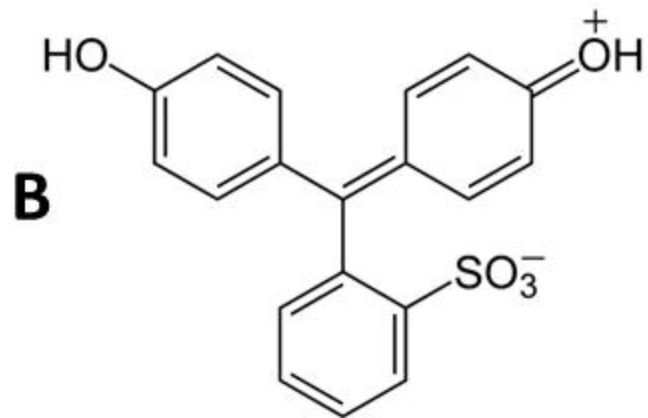
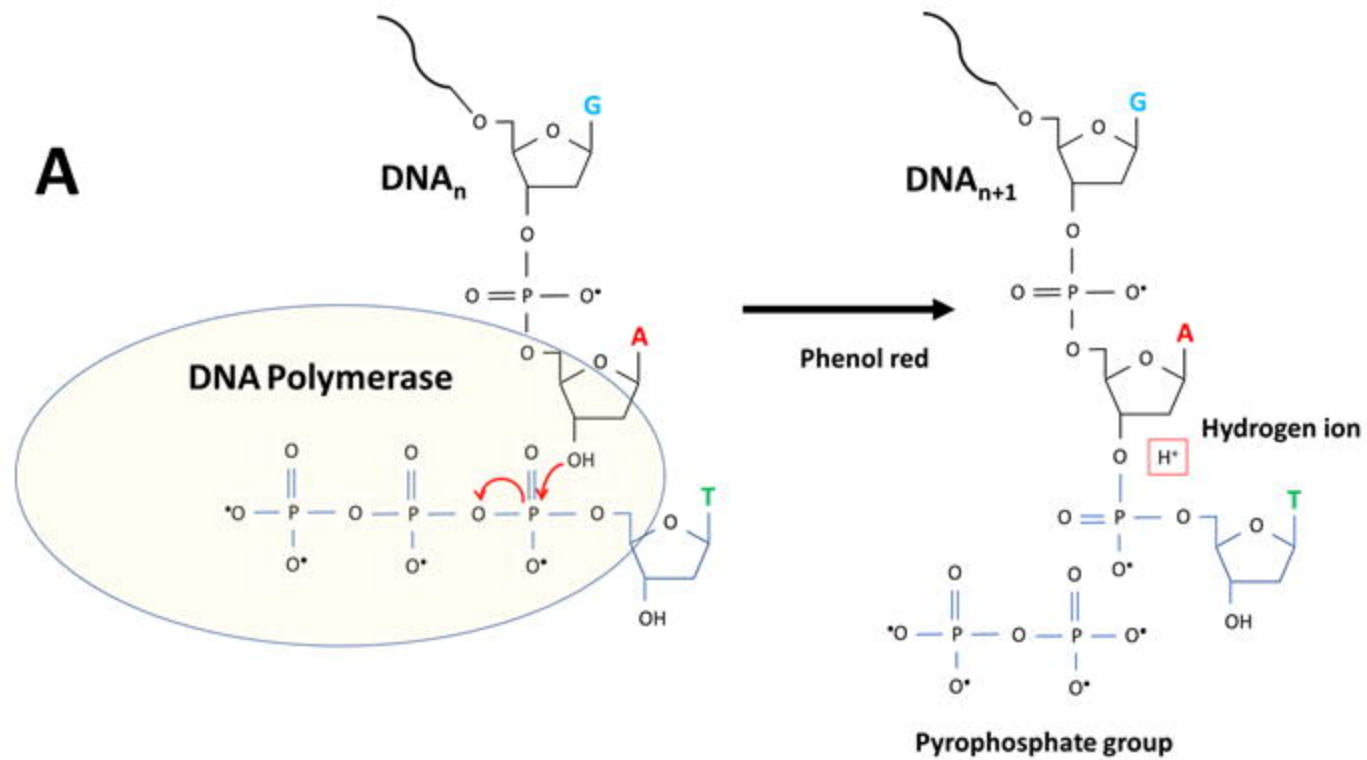


C



D





← Increasing viral copies →

A

2×10^5 4×10^4 1×10^4 2.5×10^3 625

Set α

Negative

Set β

B

Set α

1 2 3 4 5 6 7

C

Set β

1 2 3 4 5 6 7

